Restriction to gene flow is associated with changes in the molecular basis of pyrethroid resistance in the malaria vector *Anopheles funestus*

Kayla G. Barnes[a,b,c], Helen Irving[a], Martin Chiumia[d], Themba Mzilahowa[d], Michael Coleman[a], Janet Hemingway[a,1], and Charles S. Wondji[a,e,1]

[a]Department of Vector Biology, Liverpool School of Tropical Medicine, Liverpool L3 5QA, United Kingdom; [b]FAS Center for Systems Biology, Department of Organismic and Evolutionary Biology, Harvard University, Cambridge, MA 02138; [c]Broad Institute, Cambridge, MA 02142; [d]Malaria Alert Centre, College of Medicine, University of Malawi, Blantyre 3, Malawi; and [e]LSTM/OCEAC Research Unit, Organisation de Coordination pour la lutte contre les Endémies en Afrique Centrale, BP 288 Yaoundé, Cameroon

Contributed by Janet Hemingway, November 11, 2016 (sent for review June 20, 2016; reviewed by Rahindra Abeyasinghe and Joshua Yukich)

Resistance to pyrethroids, the sole insecticide class recommended for treating bed nets, threatens the control of major malaria vectors, including *Anopheles funestus*. Effective management of resistance requires an understanding of the dynamics and mechanisms driving resistance. Here, using genome-wide transcription and genetic diversity analyses, we show that a shift in the molecular basis of pyrethroid resistance in southern African populations of this species is associated with a restricted gene flow. Across the most highly endemic and densely populated regions in Malawi, *An. funestus* is resistant to pyrethroids, carbamates, and organochlorides. Genome-wide microarray-based transcription analysis identified overexpression of cytochrome P450 genes as the main mechanism driving this resistance. The most up-regulated genes include cytochrome P450s (*CYP*) *CYP6P9a*, *CYP6P9b* and *CYP6M7*. However, a significant shift in the overexpression profile of these genes was detected across a south/north transect, with *CYP6P9a* and *CYP6P9b* more highly overexpressed in the southern resistance front and *CYP6M7* predominant in the northern front. A genome-wide genetic structure analysis of southern African populations of *An. funestus* from Zambia, Malawi, and Mozambique revealed a restriction of gene flow between populations, in line with the geographical variation observed in the transcriptomic analysis. Genetic polymorphism analysis of the three key resistance genes, *CYP6P9a*, *CYP6P9b*, and *CYP6M7*, support barriers to gene flow that are shaping the underlying molecular basis of pyrethroid resistance across southern Africa. This barrier to gene flow is likely to impact the design and implementation of resistance management strategies in the region.

malaria | pyrethroid resistance | *Anopheles funestus* | cytochrome P450 | gene flow

Vector control, including indoor residual spraying (IRS) and long-lasting insecticide- treated bed nets (LLINs), is the primary control intervention to prevent malaria transmission. Unfortunately, insecticide resistance is threatening the continued success of these crucial control tools (1). In southern African countries, such as Malawi, this is especially concerning because *Anopheles funestus*, the primary disease vector, is increasingly resistant to insecticides, although whether the resistance front is unique or gene flow is uniform across the region remains unclear. Malawi has recently experienced a scale-up of vector control interventions throughout the country, including large-scale distribution of LLINs starting in 2007 and a six-district IRS campaign starting in 2009 along the densely populated Lake Malawi and in the southern agricultural district of Chikwawa (CKW). The pyrethroid lambda cyhalothrin (ICON; Syngenta) was first used in Nkhotakota (NKK) in 2009, followed by pirimiphos methyl (Actellic 50 EC; Syngenta) in NKK and Salima (SLM) in 2010 and again in NKK in 2011. Simultaneously, insecticide resistance was documented in the southern agricultural area of CKW, where lambda cyhalothrin was being used for IRS, as well as in the isolated Likoma Island in Lake Malawi (2, 3), but the insecticide resistance status of *An. funestus* in the rest of the country was largely unknown. Therefore, an extensive susceptibility profiling of local vector populations spanning the most endemic districts in Malawi is needed to design appropriate control strategies and to assess whether the strategies being deployed are sustainable nationwide and throughout southern Africa, where *An. funestus* dominates.

Previous investigation of pyrethroid resistance in southern Africa has revealed an absence of the knockdown resistance (*kdr*) target site mutation (3–5). Instead, pyrethroid resistance in *An. funestus* is driven mainly by metabolic mechanisms, primarily through overexpression of the tandemly duplicated cytochrome P450s (*CYP*) *CYP6P9a* and *CYP6P9b*, located on the *rp1* pyrethroid resistance quantitative trait locus (QTL) (5, 6). Recently, the contribution of *CYP6M7* to pyrethroid resistance in southern Africa was confirmed, with a more predominant role for this gene reported in Zambia than in Mozambique (4), raising the possibility that the molecular basis of pyrethroid resistance might vary across southern African populations. If such a shift exists, the underlying factors behind such differences remain uncharacterized.

Significance

Vector control is the cornerstone of malaria prevention. Wide-scale distribution of treated bed nets and indoor residual spraying throughout Africa has led to a major decrease in mortality, but insecticide resistance threatens this ongoing success. Here we show that across a highly endemic country, one of the main malaria vectors, *Anopheles funestus*, is resistant to several insecticide classes, including the insecticides used for bed nets. This study shows that multiple *CYP450s*, genes linked to xenobiotic metabolism, are responsible for insecticide resistance, but their impact varies significantly depending on geography. Genetic diversity analysis revealed that this genomic variation is associated with barriers to gene flow between southern African populations of *An. funestus*. This work should help improve resistance management and vector control strategies throughout southern Africa.

Author contributions: C.S.W. designed research; K.G.B., H.I., M. Chiumia, and T.M. performed research; M. Coleman contributed new reagents/analytic tools; K.G.B., J.H., and C.S.W. analyzed data; and K.G.B., J.H., and C.S.W. wrote the paper.

Reviewers: R.A., World Health Organization; and J.Y., School of Public Health and Tropical Medicine, Tulane University.

The authors declare no conflict of interest.

Freely available online through the PNAS open access option.

Data deposition: Microarray data from this study have been deposited in ArrayExpress (accession no. E-MTAB-3342), and the DNA sequences reported in this paper have been deposited in GenBank (accession nos. KP984806–KP984983).

[1]To whom correspondence may be addressed. Email: janet.hemingway@lstmed.ac.uk or charles.wondji@lstmed.ac.uk.

This article contains supporting information online at www.pnas.org/lookup/suppl/doi:10.1073/pnas.1615458114/-/DCSupplemental.

Bordering both Mozambique and Zambia, Malawi is ideally located for testing the hypothesis that the mechanisms of pyrethroid resistance vary across this region, and that this difference is linked to the genetic structure of *An. funestus* throughout southern Africa. In addition, it remains possible that the screening of new populations also could detect new genes driving such resistance. Identifying the full set of genes involved in resistance will help decipher the molecular basis of resistance and potentially identify suitable resistance markers to explain the total genetic variance of pyrethroid resistance, which can be used in the design of DNA-based molecular diagnostic tools for readily detecting and tracking resistance in the field.

Here, using genome-wide transcription and genetic diversity analyses, we show that a shift in the molecular basis of pyrethroid resistance in southern African populations of *An. funestus* is associated with significant reduced gene flow levels between southern and northern populations of this region. Previously it was thought that P450s located in the *rp1* were mainly responsible for pyrethroid resistance, and although they play a key role in insecticide metabolism, genes located on other chromosomes, mainly *CYP6M7* on the 2L chromosome, are important as well. Therefore, diagnostic assays for insecticide resistance need to incorporate a multigene panel. In addition, this work provides evidence that population structure and variation in gene expression are correlative and can be used to inform future interventions, especially as new insecticides come to market.

Results

Insecticide Resistance Profile of *An. funestus* Across Malawi. The mortality rates of all three districts chosen to span the highly endemic region of Malawi (Fig. 1*A*) showed high resistance to the pyrethroids permethrin (32–43% mortality rate) and deltamethrin (16–40%) and to the carbamate bendiocarb (32–58%), with moderate resistance to dichlorodiphenyltrichloroethane (DDT) (76–85%) (Fig. 1*B*). In contrast, there was full susceptibility to the organophosphate malathion (100%), as reported previously for this species in other African locations (7). Pre-exposure of mosquitoes to piperonyl butoxide (PBO), a synergist assay that inhibits P450 activity, followed by exposure to permethrin and bendiocarb, restored full susceptibility to both insecticides (100% mortality) in all three populations, suggesting that cytochrome P450s are driving resistance to carbamates and pyrethroids.

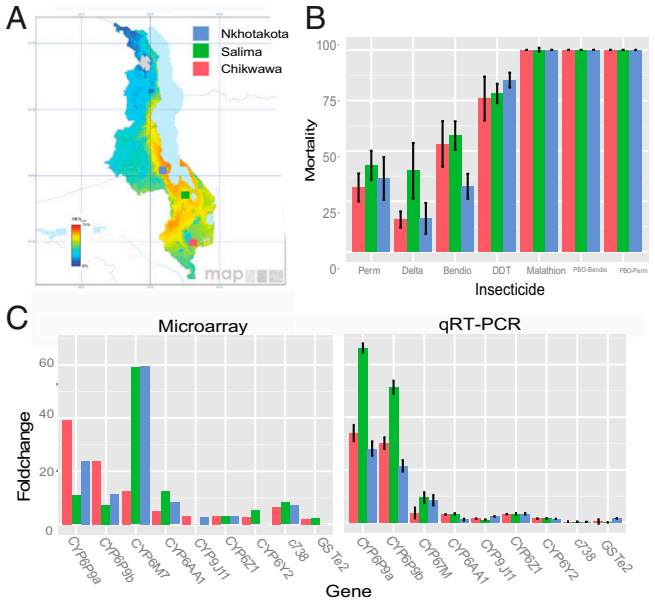

Fig. 1. Insecticide resistance and gene expression profiling. (*A*) Map of malaria incidence levels at Malawi collection sites: Chikwawa (CKW), Salima (SLM), and Nkhotakota (NKK). (*B*) Susceptibility profile of Malawian *An. funestus* population to the main insecticides and a synergist (PBO). Data are mean ± SEM values of 185–200 mosquitoes (100 for malathion). (*C*) Fold change determined using microarray and qRT-PCR analyses. For qRT-PCR, error bars represent SD.

Genome-Wide Transcription Profiling of Pyrethroid Resistance. Mosquitoes resistant to permethrin, unexposed to insecticide, and of a susceptible laboratory strain (FANG) were used to analyze the transcriptome profile. The set of genes differentially expressed (i.e., a greater than twofold change; $P < 0.05$) for each comparison of resistant (R) vs. susceptible (S) (Fig. 1*C*) and unexposed control (C) vs. S (*SI Appendix*, Fig. S1*D*) were determined for each location and between the locations. The three districts in Malawi share 192 overtranscribed probes [fold change (FC) ≥2; $P < 0.01$] (*SI Appendix*, Fig. S1*A*). Additional probes were overtranscribed in only two collection sites (CKW-NKK, 302 probes; NKK-SLM, 100 probes; SLM-CKW, 229 probes), whereas other probes were specific to a single location.

The list of genes commonly overexpressed across Malawi comprises several gene families, among which the most preeminent were the cytochrome P450 genes (*SI Appendix*, Table S1). Similar to previous reports for southern Africa, the most highly overexpressed of these P450s in all three locations in Malawi belong to the CYP6 family, including *CYP6P9a*, *CYP6P9b*, and *CYP6M7* (4, 5, 8). Contrary to previous reports, here the overexpression of these candidate genes shows significant geographical variation between southern and northern districts. In CKW, *CYP6P9a* (FC, 39.4) and *CYP6P9b* (FC, 23.96) have the highest overexpression levels, whereas a lower fold change is observed for *CYP6M7* (FC, 12.5) (Fig. 1*C*) The opposite pattern is observed in the northern districts, where *CYP6M7* has the highest expression in SLM (FC: *CYP6P9a*, 8.37; *CYP6P9b*, 8.6; *CYP6M7*, 59.06) and NKK (FC: *CYP6P9a*, 13.75; *CYP6P9b*, 11.33; *CYP6M7*, 59.63). This shift in expression pattern was also observed for other cytochrome P450s commonly overexpressed in all three locations. These include *CYP6AA1* located on the *rp1* pyrethroid resistance QTL, with greater overexpression in northern locations (FC: SLM, 12.66; NKK, 8.25; CKW, 5.20), and *CYP6M4*, exhibiting greater expression in the south (FC: CKW, 12.45; SLM, 3.82; NKK, 3.51). Another P450 from the CYP4 family, *CYP4C27*, was highly overexpressed in the two northern locations of SLM (FC, 19.50) and NKK (FC, 26.78) but minimally overexpressed in the southern location of CKW (FC, 2.11). Other P450 genes, such as *CYP6Z1*, had a similar expression in all three locations (FC: SLM, 3.01; NKK, 2.95; CKW, 3.04) (*SI Appendix*, Table S1). Beside cytochrome P450s, other genes belonging to multiple gene families included several proteases, and alcohol and glucose dehydrogenases were up-regulated. Although these genes may be playing a role in insecticide resistance, they are likely secondary factors, given that the PBO synergist assay established the importance of P450s in relationship to resistance. Some additional detoxifying genes were up-regulated in only one or two locations, including some P450s, with a larger set in southern Malawi, although these all exhibited a lower fold change (FC, 6.78–2.11) than the main genes of interest.

Resistance Genes Are Constitutively Overexpressed. The expression profile obtained by comparing control mosquitoes unexposed to insecticides (C) collected from the same three districts with the FANG susceptible strain (C-S) revealed that the main genes detected in R-S hybridization are also overexpressed in C-S hybridization. This finding confirms that these genes are constitutively overexpressed in resistant mosquitoes and are not induced by insecticide exposure. The expression profile of C-S is presented in *SI Appendix*, Table S1. The geographical shift in gene expression of key resistance genes identified using the R-S comparison was also confirmed using the C-S comparison, with greater overexpression of *CYP6M7* (FC: SLM, 41.11; NKK, 24.08; CKW, 3.73) found in the northern sites and greater overexpression of *CYP6P9a* (FC: SLM, 7.00; NKK, 7.17; CKW, 69.19) and *CYP6P9b* (FC: SLM, 8.85; NKK, 6.56; CKW, 26.56) seen in the southern site.

Validation of Overtranscription with qRT-PCR. Quantitative real-time PCR (qRT-PCR) analysis broadly confirmed the microarray results for the seven genes tested, with a significant correlation observed between qRT-PCR and microarray fold change results ($R^2 = 0.519$), although some variation between the techniques was observed (*SI Appendix*, *Results* and Fig. S1*B*).

Analysis of Genetic Diversity Across Southern Africa. The significant differences in the gene expression profiles observed between populations of *An. funestus* in Malawi complement previously reported differences in expression profiles between Zambia and Mozambique (4). These variations could suggest the presence of barriers to gene flow that are affecting the spread of resistance genes. Any barriers to gene flow across Malawi and throughout southern Africa could significantly impact both the speed and spread of insecticide resistance-mediating genes. Unfortunately, however, knowledge of the population structure of *An. funestus* in southern Africa is limited.

We analyzed the population structure of southern Africa using microsatellites for multiple sites in Zambia ($n = 3$), Malawi ($n = 3$), and Mozambique ($n = 1$). Field-caught female mosquitoes ($n = 36$–48) from the seven collections were typed using 17 microsatellite markers spanning the genome. The 17 microsatellite markers spanning the entire genome were genotyped consistently in all populations, demonstrating robustness of the multiplex design. Each population analyzed contained ≥36 individuals (≥72 alleles), which is sufficient for accurately estimating allele frequencies (9). The loci FUNR, FUNQ, and AFND12 showed an excess of one allele. FUNR is located in the *rp1* resistance to permethrin QTL and may be under selection. FUNQ and AFND12 are located on the X chromosome, where a loss of diversity was also identified in *An. funestus* in the African-wide analysis (10). Between four and seven total alleles were typed for each microsatellite marker.

Individual microsatellite markers were analyzed for Hardy–Weinberg equilibrium (HWE) with Bonferroni correction for multiple tests. A total of 21 out of 152 markers (13.8%) deviated from HWE owing to a deficit of heterozygosity (*SI Appendix*, Table S3). To ensure that deviation from HWE did not affect the predicted population structure, we performed all analyses on the full panel of 17 microsatellites, 14 microsatellites minus homogenous markers, and the 11 microsatellites with no HWE deviation in any population (*SI Appendix*, Table S4). We observed no linkage disequilibrium (LD). For all populations, we made a total 1,224 pairwise comparisons, of which 31 comparisons were in significant LD ($P < 0.05$), constituting <5% of alleles.

Patterns of genetic differentiation based on pairwise fixation index (F_{st}) estimates among all locations reveal the presence of a north-south geographical subdivision. Three Zambia collections plus SLM and NKK from Malawi show very low and nonsignificant F_{st} pairwise estimates, suggesting a high level of gene flow between these populations (F_{st}, 0.0001–0.04); however, significant F_{st} pairwise estimates are seen between the southern Malawi populations of CKW and populations from northern Malawi and Zambia (F_{st}, 0.0597–0.0704) and Mozambique (F_{st}, 0.0676–0.0812), suggesting the presence of barriers to gene flow (*SI Appendix*, Table S5). This genetic differentiation pattern remained after removal of the six markers deviating from HWE. The segregation in the Mozambique population (1,500 km away from Malawi) may be explained by distance, but segregation by distance breaks down when comparing western Zambia and central Malawi (*SI Appendix*, Fig. S1*C*). Western Zambia is almost 1,200 km from central Malawi yet presents as an interbreeding population, whereas southern Malawi is only 350 km from central Malawi and shows significant genetic deviation, further suggesting the presence of barriers to gene flow across Malawi.

The population structure in southern Africa is also supported by a neighbor-joining tree with genetic distances based on F_{st} estimates (Fig. 2*A*), showing a cluster of Zambian and central and northern Malawian populations, but divergence in CKW and southern Mozambique. To confirm the estimated genetic differences inferred based on F_{st}, we performed Bayesian predictions of population structure (without predefined populations based on geographically collected samples) using the full panel of 17 microsatellites. The "true" population size was $K = 3$, predicted using the Evanno method, and the graphical structure was produced for $K = 3$–7 to visualize the multimodality within and between populations. Complementary to the F_{st} predictions, the Zambia samples and the SLM and NKK samples from Malawi share a similar pattern (Fig. 2*B*).

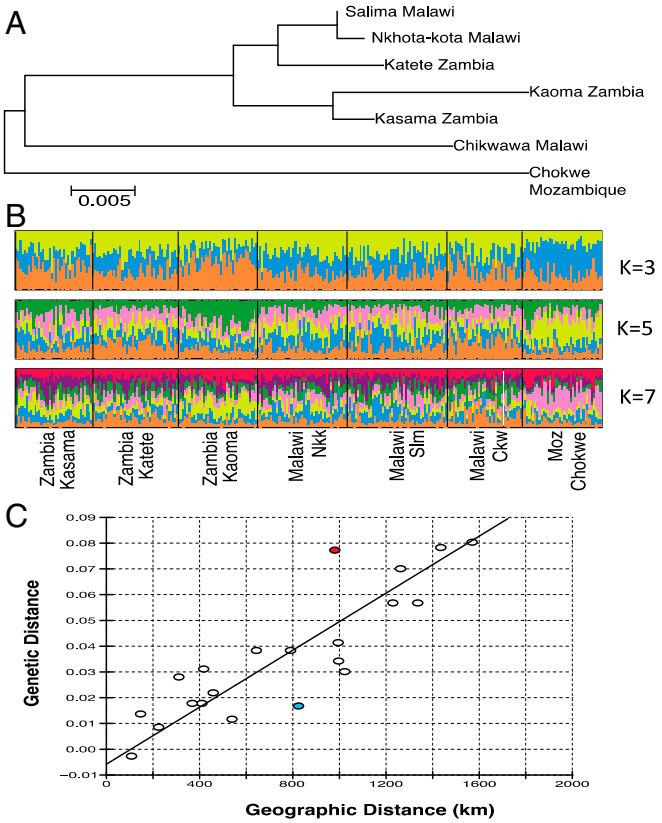

Fig. 2. Population structure of southern Africa. (*A*) Neighbor-joining tree based on the F_{st} pairwise scores using 17 microsatellites. (*B*) Bayesian-based structure patterns of southern Africa. $K = 3$, 5, 7 shows the separation of CKW, Malawi and Chokwe, Mozambique. (*C*) Isolation by distance comparing genetic distance versus geographical distance based on the Mantel test and logged scaled. The two outliers are: red dot, Ckw vs. Moz; and blue dot, west vs. north Zambia.

Genetic Diversity Patterns of *CYP6P9a*, *CYP6P9b*, and *CYP6M7* Across Malawi. We investigated the polymorphism patterns of the three main resistance genes, *CYP6P9a*, *CYP6P9b*, and *CYP6M7*, to assess for associations with the shifts in gene expression profiles across the south/north transect in Malawi, the idea being that if there is indeed a potential decreased role of *CYP6P9a* and *CYP6P9b* (both located on the *rp1* QTL) in the north, this would be reflected by a weaker signature of selection compared with that in southern Malawi. Similarly, analysis of *CYP6M7*, located on the second pyrethroid QTL, *rp2*, on the 2L chromosome, was used to further inform the selection pattern associated with pyrethroids in northern Malawi. The three genes were sequenced from resistant and susceptible mosquitoes from each district, and changes in their polymorphism pattern associated with pyrethroid resistance were analyzed.

Polymorphism Analysis of *CYP6P9a* and *CYP6P9b*. Genomic fragments of *CYP6P9a* (2,056 bp) and *CYP6P9b* (1,812 bp) were sequenced for all three locations in Malawi and analyzed with previously published sequences from Zambia and Mozambique to confirm that the polymorphic patterns observed were complementary to the trend seen throughout southern Africa (4). The sequences included the full coding region, two exons and one intron (*CYP6P9a*, 1,584 bp; *CYP6P9b*, 1,524 bp), and the 5′ UTR (*CYP6P9a*, 472 bp; *CYP6P9b*, 288 bp). In the southern district of Malawi (CKW), both

CYP6P9a and *CYP6P9b* exhibited significantly less genetic diversity in resistant mosquitoes (π: *CYP6P9a*, 0.00036; *CYP6P9b*, 0.0001) compared with susceptible mosquitoes (π: *CYP6P9a*, 0.0018; *CYP6P9b*, 0.001) (Fig. 3), low substitution numbers in resistant mosquitoes (*CYP6P9a*, 2; *CYP6P9b*, 1) compared with susceptible mosquitoes (*CYP6P9a*, 14; *CYP6P9b*, 12) (*SI Appendix*, Table S6), and a loss of haplotype diversity (*SI Appendix*, Fig. S2*A*). SLM in northern Malawi also showed reduced genetic diversity (π, resistant: *CYP6P9a*, 0.0001; *CYP6P9b*, 0.0003 vs. susceptible: *CYP6P9a*, 0.0033; *CYP6P9b*, 0.0093) and fewer substitutions (π, resistant: *CYP6P9a*, 2; *CYP6P9b*, 2 vs. resistant: *CYP6P9a*, 15; *CYP6P9b*, 52) in resistant mosquitoes compared with susceptible mosquitoes. However, in NKK, the northernmost district, both susceptible and resistant mosquitoes showed reduced genetic diversity for *CYP6P9a* (π, resistant, 0.00019 vs. susceptible, 0.00027), with only two substitutions in each phenotype and a low haplotype of 3, whereas *CYP6P9b* showed variation between resistant (π, 0.0003; S, 3) and susceptible (π, 0.0041; S, 26) mosquitoes (*SI Appendix*, Table S6).

The loss of haplotype diversity, mainly in resistant mosquitoes, is consistent throughout southern Africa. Resistant samples from Malawi, Zambia, and Mozambique show significantly reduced haplotype diversity for *CYP6P9a*, with only 10 mutational positions observed in resistant mosquitoes across the region accounting for 10 haplotypes, whereas in susceptible mosquitoes, up to 103 mutational positions are observed generating 25 haplotypes (*SI Appendix*, Figs. S3 and S4). *CYP6P9b* also shows a similar loss in diversity in resistant mosquitoes, with nine mutations leading to only 10 haplotypes in resistant mosquitoes, but up to 100 mutational positions generating 20 haplotypes in susceptible mosquitoes.

The significant differences in polymorphism patterns of resistant and susceptible mosquitoes were also observed at the protein level, with key amino acid changes detected that likely impact the metabolic efficacy of both enzymes toward pyrethroids, as demonstrated recently (11) (*SI Appendix*, *Results*).

Although the pattern of reduced diversity in resistant mosquitoes is consistent throughout southern Africa, there is evidence of geographical variation in these genes. The predominant haplotype (H1) in *CYP6P9a* and *CYP6P9b* is consistently more prevalent in southern Malawi (CKW: 90% and 95%, respectively) and Mozambique (90% and 90%) compared with cluster 1, SLM (70% and 55%), NKK (75% and 60%), and west Zambia (70% and 40%) (Fig. 4). The TCS (Templeton, Crandall and Sing) network reveals that *CYP6P9a* and *CYP6P9b* haplotypes from CKW are separated by fewer than five mutational steps, whereas haplotypes from SLM and NKK have more mutational steps (>12–20). For *CYP6P9b*, there is an obvious geographic shift, with all singleton haplotypes obtained from the northern locations (13 of 40 haplotypes). Most of these alleles are *CYP6P9b*-susceptible haplotypes, with a few resistant alleles divergent from the H1 and H2R haplotypes. In the north, there are several other resistant haplotypes separated by only a single mutational step from the predominant H1 haplotypes.

The greater diversity of *CYP6P9a* in northern Malawi is confirmed by a maximum likelihood (ML) tree in which several haplotypes from SLM and NKK form an independent cluster with greater genetic distance from the predominant haplotype (*SI Appendix*, Fig. S4*A*). There is one major clade for both *CYP6P9a* and *CYP6P9b* composed mainly of resistant sequences and small divergent clades representing susceptible sequences (*SI Appendix*, Fig. S4 *A* and *B*). The ML tree shows that sequences from southern Mozambique cluster closer to those from southern Malawi, and sequences from Zambia cluster with those from northern Malawi. This pattern of diversity further supports the presence of a shift in gene expression of these two important pyrethroid resistance genes across southern Africa. A sliding-window analysis of the nucleotide diversity across the full-length of *CYP6P9a* and *CYP6P9b* showed that the loss of diversity is not restricted to the 5′ UTR or introns, with significant loss of diversity also seen throughout the coding region of resistant mosquitoes compared with susceptible mosquitoes in all three locations (*SI Appendix*, Fig. S4 *D* and *E*).

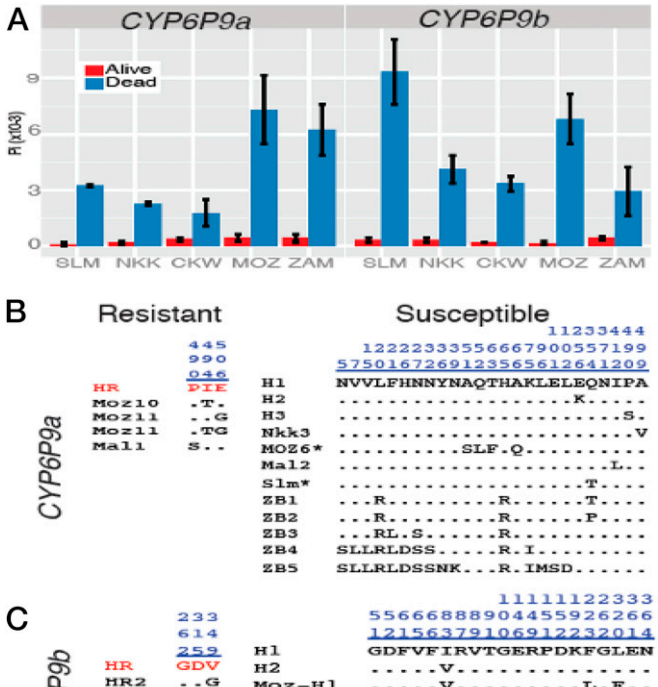

Fig. 3. Haplotype distribution analysis of *CYP6P9a* and *CYP6P9b*. (*A*) Nucleotide diversity based on Pi × 10^{-3} for *CYP6P9a* and *CYP6P9b*. Significance between resistant (red) and susceptible (blue), including SD: **P* < 0.05; ***P* < 0.01. (*B* and *C*) The polymorphic amino acid positions for both *CYP6P9a* and *CYP6P9b*, respectively, between resistant and susceptible individuals. Three locations in Malawi (CKW, Chikwawa; SLM, Salima; and NKK, Nkhotakota), one location in Mozambique (MOZ), and one location in Zambia (ZB). H denotes haplotypes from more than one location. Blue numbers on the top *x*-axis are the amino acid position. For resistant amino acids, the susceptible amino acid is listed in red.

Polymorphism Analysis of *CYP6M7*. Sequencing of a 1.2-kb genomic fragment spanning the 5′ UTR (610 bp) and first exon (590 bp) between five resistant (alive after 1 h) and five susceptible (dead after 1 h) individual mosquitoes per site revealed a high genetic diversity in *CYP6M7*, with no correlation with either the resistance phenotype or geographical location (*SI Appendix*, Table S7). In contrast to *CYP6P9a* and *CYP6P9b*, there is high haplotype diversity (0.9–1) (*SI Appendix*, Fig. S2*A*), high nucleotide diversity (π, 0.01–0.02), and no dominant haplotype in Malawi or throughout southern Africa. The TCS network shows no phenotypic grouping in Malawi, and 90% of samples have a unique haplotype (Fig. 4). Analysis of individual samples using a ML tree showed that resistant and susceptible mosquitos are equally diverse and divergent, with no phenotypic clustering (*SI Appendix*, Fig. S4). Analysis of Tajima's *D* (combined, −0.64; resistant, −0.07; susceptible, −0.41) and Fu and Li's *D** (combined, 0.78; resistant, 0.43; susceptible, 1.27) estimates did not uncover any evidence indicating that *CYP6M7* is under selection (*SI Appendix*, Table S7). Closer analysis of the 5′ UTR and coding region of *CYP6M7* revealed little difference in Hd (haplotype diversity) estimates, either geographically or phenotypically, between resistant and susceptible mosquitoes.

Discussion

Insecticide resistance threatens malaria control interventions in Africa, particularly in a number of highly endemic countries in southern Africa. Coherent vector management plans are needed to access bilateral and international support for malaria control.

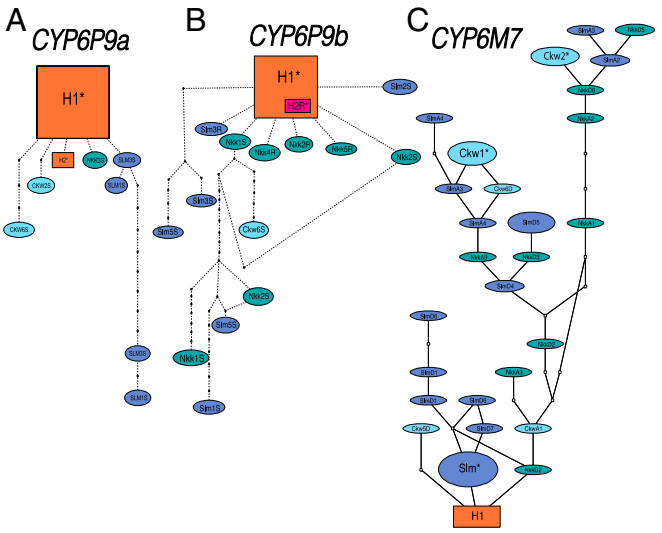

Fig. 4. Comparative analysis of haplotype diversity across Malawi. A TCS network was constructed for the coding region for all samples from Malawi (light blue, CKW; green, NKK; blue, SLM) for *CYP6P9a* (*A*), *CYP6P9b* (*B*), and *CYP6M7* (*C*). Haplotypes with multiple hits are denoted by "H," and resistance haplotypes are orange squares. Unique haplotypes are shown as circles with sample information, including a three-digit location code and designation as susceptible (S) or resistant (R).

Designing and implementing such plans requires knowledge of the resistance profiles of major malaria vectors to the available insecticides, as well as the elucidation of underlying resistance mechanisms to develop better insecticide resistance diagnostics and future insecticides. To help achieve such goals, this study has established the resistance profile of *An. funestus* on a south/central transect in Malawi, which encompasses the most densely populated areas of Malawi with the highest incidence of malaria, and detected a geographical shift in the resistance mechanisms corresponding to patterns of population structure throughout southern Africa.

Widespread Distribution of Insecticide Resistance Is a Concern for Malaria Control. *An. funestus* populations across Malawi are resistant to pyrethroids, which is of concern given that pyrethroids are the sole insecticide class currently recommended by the World Health Organization (WHO) for use on bed nets. This concern is increased by the presence of resistance to the carbamate bendiocarb, the main alternative to pyrethroids for IRS. The resistance profile described in this study confirms resistance in isolated districts in Malawi (3, 12) and is similar to that in neighboring countries, including Mozambique (13, 14) and Zambia (4, 8), suggesting that pyrethroid and carbamate resistance is widespread in southern Africa, but the genetic mechanisms responsible for this resistance are not uniform. The apparent shift in gene expression in *An. funestus* populations observed between southern and northern locations, especially in Malawi, where geographical distance is not a factor, suggests that widespread resistance is likely the result not of a single mutational event and subsequent gene flow, but of multiple independent events.

Multiple Cytochrome P450s Are Driving Pyrethroid Resistance in Malawi, but with Geographical Variation. Despite the similar resistance levels throughout Malawi, a clear south/north geographical difference was observed in the transcription profile of the main pyrethroid resistance genes, *CYP6P9a* and *CYP6P9b*, under directional selection but more significantly in southern Malawi. Such geographical differences in the role of key metabolic resistance genes have also been observed in the *An. gambiae* genes *CYP6M2* and *CYP6P3* (15, 16), as well as in several CYP9 genes in *Aedes aegypti* (17).

In contrast to *CYP6P9a* and *CYP6P9b*, no evidence of selection was detected for *CYP6M7*, and it is likely that the molecular basis through which *CYP6M7* confers pyrethroid resistance differ from that of *CYP6P9a* and *CYP6P9b*, with little contribution from polymorphisms from coding regions. The overtranscription of *CYP6M7* may be caused by changes in the gene's promoter region or by mutations in the transcription factors. Further work is needed to fully elucidate the mechanism driving overexpression in *CYP6M7*. The highly polymorphic nature of *CYP6M7* indicates that no selective pressure is acting on this gene, even though it is highly overexpressed and linked to pyrethroid resistance throughout the region (4, 8). The elevated expression of *CYP6M7* in northern Malawi and Zambia suggests the likely presence of two resistance fronts in southern Africa.

The finding of geographical differences in the role of key resistance genes in Malawi suggests the presence of barriers to gene flow or variation in selection forces between populations from south to north. Previous work predicted that southern Africa was one interbreeding population based on continent-wide analysis (18), but genome-wide genetic diversity analysis using F_{st} comparisons and Bayesian structure analysis has revealed three population clusters in southern Africa. Cluster 1, which includes Zambia and northern Malawi (SLM and NKK), corresponds to greater overexpression of *CYP6M7*. Southern Malawi forms a unique cluster (cluster 2), likely owing to its location at the end of the Rift Valley, which has previously been shown to constitute a barrier to gene flow in the other major malaria vector, *An. gambiae* (19). The difference in gene expression profiles between southern and northern Malawi further supports the presence of barriers to gene flow. Mozambique (cluster 3) lies >1,500 km from southern Malawi, and the level of genetic differentiation observed with southern Malawi could be a consequence of an isolation by distance, as suggested by our analysis (Fig. 2*C*). A similar expression profile between southern Malawi and Mozambique further supports the role of isolation by distance (Fig. 2*C*). Future studies with wider sampling across the southern Africa region will help further define patterns of gene flow in *An. funestus* and other malaria vectors, increase the number of genetic markers identified, and, using new next-generation sequencing tools, such as ddRADseq and whole-genome sequencing, further elucidate the genetic structure of this malaria vector in southern Africa.

The finding of differences in the molecular basis of resistance within a given country means that national resistance management strategies without characterization of underlying resistance mechanisms from multiple localities may be flawed. The similarity of resistance profiles in Malawian *An. funestus* suggests that the same resistance management strategy could be implemented nationally, although attention should be given to the independent evolution of resistance mechanisms across the region. The full susceptibility against organophosphate suggests that an IRS campaign using an insecticide from this class, such as pirimiphos methyl, could be a viable alternative, although the higher cost and lower residual efficacy of this insecticide could be a limiting factor. This was seen when pirimiphos methyl was sprayed for 2 y in NKK and 1 y in SLM and showed low efficiency after 2 mo. This may explain some of the differences in gene expression profiles in central Malawi vs. southern Malawi, but does not explain the elevated overexpression of *CYP6M7* observed in Zambia, a country that has used mainly pyrethroid and carbamate insecticides for IRS. Overall, the predominant role of cytochrome P450s in pyrethroid resistance in Malawi suggests that rolling out the new generation of bed nets that combine pyrethroids and a P450 inhibitors (20) could improve LLIN effectiveness across this region. Most importantly, this study supports the view that pyrethroids should be eliminated from IRS use to prevent resistance from becoming fixed.

Broadly, this study highlights the major role of cytochrome P450s in pyrethroid resistance; however, the underlying molecular basis of resistance in one area does not necessarily extend to other regions, a property that should be considered when designing resistance management strategies. The role of P450s in resistance is not limited to *An. funestus*. Cytochrome P450s have been linked to insecticide resistance in other major malaria vectors, including *An. gambiae* (21) and *Anopheles minimus* (22), as well as the major

Dengue virus and Zika virus vector *Aedes aegypti* (17, 23). In addition, many agricultural pests, including aphids (24), whiteflies (25), and plant hoppers (26), use the expression of multiple P450s to metabolize pesticides. Understanding the population structure of a species can help inform potential genetic differences in resistance and the breath of sampling needed to determine mechanisms driving this resistance. As existing insecticides and pesticides are scaled up, and as new insecticides and pesticides reach the public market, molecular studies of multiple collections are needed to fully elucidate the mechanisms of resistance to ensure the longevity of both vector and pest control.

Methods

Mosquito Collection and Insecticide Bioassays. Gravid indoor resting female mosquito collections were carried out in three highly endemic districts: CKW, SLM, and NKK (Fig. 1*A*). Three to five collections at each site were conducted over two rainy seasons, November 2010–February 2011 and November 2011–February 2012. Two seasonal collections were needed to generate adequate numbers to test the full spectrum of insecticides. Eggs were collected, and female F0 mosquitoes used for oviposition were species-identified using *funestus* complex mixture PCR (27). Insecticide resistance was assessed using 2- to 5-d-old F1 adult mosquitoes. Standardized WHO insecticide-impregnated papers were used for all experiments including the 4% PBO. The 1-h bioassays for the insecticides 0.1% bendiocarb (carbamate), 4% DDT (organochlorine), 0.05% deltamethrin (pyrethroid), 0.75% permethrin (pyrethroid), and 5% malathion (organophosphate) were carried out following methods detailed in the WHO manual (28) using 185–200 adult females and 100–150 adult males plus parallel control tubes. Resistant mosquitoes (alive after 24 h) were stored at −80 °C, and dead mosquitoes were stored on silica gel. Mosquitos were collected from Zambia in 2009 and 2010 (29) and from Mozambique in 2009 (14) (*SI Appendix*, Fig. S5).

Microarray and qRT-PCR. Thirty custom 8 × 60K Agilent microarrays (A-MEXP-2374) (4) were used to analyze the genome-wide transcription profile for the three locations. RNA was extracted from three pools of 10 female mosquitoes per location per phenotype: C (unexposed to insecticide), R (resistant after exposure to 0.75% permethrin), and S (susceptible colony; FANG) (30), using the Picopure RNA Isolation Kit (Applied Biosystems). Transcription profiles where determined using Genespring GX 12.0 software. cDNA was synthesized from four biological replicates for R, C, and S mosquitoes per district and carried out as described previously (15). Fold change was calculated using three technical replicates and normalizing with two housekeeping genes, Actin and SP7, using the $2^{-\Delta\Delta CT}$ method (31).

Genetic Population Structure of *An. funestus* in Southern Africa. Seventeen microsatellites spanning the genome were optimized and genotyped into three plexes (*SI Appendix*, Table S2) for Zambia ($n = 3$), Malawi ($n = 3$), and Mozambique ($n = 1$). Then 48 gDNA samples from each population ($n = 432$) were run using the Type-it Microsatellite PCR Kit (Qiagen) and scored. HWE, LD, F-statistics, null-allele, and F_{st} were determined using GENEPOP 4.0.10 (32). Bayesian analysis of population structure was generated using STRUCTUREv2 (33). The genetic distance (determined by pairwise F_{st} score) was compared with geographical distance using isolation by distance (34).

Genetic Variability of Candidate Genes. For the resistance genes of interest, *CYP6P9a*, *CYP6P9b*, and *CYP6M7*, the full-length coding region as well as the 5′ UTR were amplified in all three districts in Malawi. gDNA was extracted on five resistant and five susceptible female F1 mosquitoes using the Livak DNA extraction method or the DNAeasy Kit (Qiagen). Amplification followed previously published methods (6). Aligned sequences were haplotype-phased, the coding regions were defined using Blastx, and genetic parameters were determined using dnaSP 5.1 (35).

Details of our analysis are provided in *SI Appendix, Materials and Methods*. All DNA sequences in this study have been deposited in the GenBank database (accession nos. KP984806–KP984983), and all microarray data have been submitted to Array Express (accession no. E-MTAB-3342).

ACKNOWLEDGMENTS. This work was supported by Wellcome Trust Research Career Development Fellowship 083515/Z/07/Z and Senior Research Fellowship 101893/Z/13/Z (to C.S.W.) and by National Institutes of Health Grant IU01 A1058271-01 (to J.H.).

1. World Health Organization (2012) *Global Plan for Insecticide Resistance Management (GPIRM)* (World Health Organization, Geneva, Switzerland).
2. Hunt R, Edwardes M, Coetzee M (2010) Pyrethroid resistance in southern African *Anopheles funestus* extends to Likoma Island in Lake Malawi. *Parasit Vectors* 3:122.
3. Wondji CS, et al. (2012) Impact of pyrethroid resistance on operational malaria control in Malawi. *Proc Natl Acad Sci USA* 109(47):19063–19070.
4. Riveron JM, et al. (2014) The highly polymorphic CYP6M7 cytochrome P450 gene partners with the directionally selected *CYP6P9a* and *CYP6P9b* genes to expand the pyrethroid resistance front in the malaria vector *Anopheles funestus* in Africa. *BMC Genomics* 15(1):817.
5. Riveron JM, et al. (2013) Directionally selected cytochrome P450 alleles are driving the spread of pyrethroid resistance in the major malaria vector *Anopheles funestus*. *Proc Natl Acad Sci USA* 110(1):252–257.
6. Wondji CS, et al. (2009) Two duplicated P450 genes are associated with pyrethroid resistance in *Anopheles funestus*, a major malaria vector. *Genome Res* 19(3):452–459.
7. Coetzee M, Koekemoer LL (2013) Molecular systematics and insecticide resistance in the major African malaria vector *Anopheles funestus*. *Annu Rev Entomol* 58:393–412.
8. Thomsen EK, et al. (2014) Underpinning sustainable vector control through informed insecticide resistance management. *PLoS One* 9(6):e99822.
9. Hale ML, Burg TM, Steeves TE (2012) Sampling for microsatellite-based population genetic studies: 25 to 30 individuals per population is enough to accurately estimate allele frequencies. *PLoS One* 7(9):e45170.
10. Temu EA, Hunt RH, Coetzee M (2004) Microsatellite DNA polymorphism and heterozygosity in the malaria vector mosquito *Anopheles funestus* (Diptera: Culicidae) in east and southern Africa. *Acta Trop* 90(1):39–49.
11. Ibrahim SS, et al. (2015) Allelic variation of cytochrome P450s drives resistance to bednet insecticides in a major malaria vector. *PLoS Genet* 11(10):e1005618.
12. Vezenegho SB, et al. (2013) Characterization of the *Anopheles funestus* group, including *Anopheles funestus*-like, from northern Malawi. *Trans R Soc Trop Med Hyg* 107(12):753–762.
13. Casimiro S, Coleman M, Mohloai P, Hemingway J, Sharp B (2006) Insecticide resistance in *Anopheles funestus* (Diptera: Culicidae) from Mozambique. *J Med Entomol* 43(2):267–275.
14. Cuamba N, Morgan JC, Irving H, Steven A, Wondji CS (2010) High level of pyrethroid resistance in an *Anopheles funestus* population of the Chokwe District in Mozambique. *PLoS One* 5(6):e11010.
15. Kwiatkowska RM, et al. (2013) Dissecting the mechanisms responsible for the multiple insecticide resistance phenotype in *Anopheles gambiae* s.s., M form, from Vallée du Kou, Burkina Faso. *Gene* 519(1):98–106.
16. Tene Fossog B, et al. (2013) Physiological correlates of ecological divergence along an urbanization gradient: differential tolerance to ammonia among molecular forms of the malaria mosquito *Anopheles gambiae*. *BMC Ecol* 13:1.
17. Strode C, et al. (2008) Genomic analysis of detoxification genes in the mosquito *Aedes aegypti*. *Insect Biochem Mol Biol* 38(1):113–123.
18. Michel AP, et al. (2005) Rangewide population genetic structure of the African malaria vector *Anopheles funestus*. *Mol Ecol* 14(14):4235–4248.
19. Lehmann T, et al. (1999) The Rift Valley complex as a barrier to gene flow for Anopheles gambiae in Kenya. *J Hered* 90(6):613–621.
20. Strode C, Donegan S, Garner P, Enayati AA, Hemingway J (2014) The impact of pyrethroid resistance on the efficacy of insecticide-treated bed nets against African anopheline mosquitoes: Systematic review and meta-analysis. *PLoS Med* 11(3):e1001619.
21. Ranson H, et al. (2002) Molecular analysis of multiple cytochrome P450 genes from the malaria vector, *Anopheles gambiae*. *Insect Mol Biol* 11(5):409–418.
22. Rodpradit P, Boonsuepsakul S, Chareonviriyaphap T, Bangs MJ, Rongnoparut P (2005) Cytochrome P450 genes: Molecular cloning and overexpression in a pyrethroid-resistant strain of *Anopheles minimus* mosquito. *J Am Mosq Control Assoc* 21(1):71–79.
23. Ishak IH, et al. (2016) The cytochrome P450 gene CYP6P12 confers pyrethroid resistance in kdr-free Malaysian populations of the dengue vector *Aedes albopictus*. *Sci Rep* 6:24707.
24. Puinean AM, et al. (2010) Amplification of a cytochrome P450 gene is associated with resistance to neonicotinoid insecticides in the aphid *Myzus persicae*. *PLoS Genet* 6(6):e1000999.
25. Karatolos N, et al. (2012) Over-expression of a cytochrome P450 is associated with resistance to pyriproxyfen in the greenhouse whitefly *Trialeurodes vaporariorum*. *PLoS One* 7(2):e31077.
26. Bass C, et al. (2011) Overexpression of a cytochrome P450 monooxygenase, CYP6ER1, is associated with resistance to imidacloprid in the brown planthopper, *Nilaparvata lugens*. *Insect Mol Biol* 20(6):763–773.
27. Koekemoer LL, Kamau L, Hunt RH, Coetzee M (2002) A cocktail polymerase chain reaction assay to identify members of the *Anopheles funestus* (Diptera: Culicidae) group. *Am J Trop Med Hyg* 66(6):804–811.
28. World Health Organization (2013) *Test Procedures for Insecticide Resistance Monitoring in Malaria Vector Mosquitoes* (World Health Organization, Geneva, Switzerland).
29. Chanda E, et al. (2011) Insecticide resistance and the future of malaria control in Zambia. *PLoS One* 6(9):e24336.
30. Wondji CS, et al. (2005) An integrated genetic and physical map for the malaria vector *Anopheles funestus*. *Genetics* 171(4):1779–1787.
31. Schmittgen TD, Livak KJ (2008) Analyzing real-time PCR data by the comparative C(T) method. *Nat Protoc* 3(6):1101–1108.
32. Rousset F (2008) genepop'007: A complete re-implementation of the genepop software for Windows and Linux. *Mol Ecol Resour* 8(1):103–106.
33. Pritchard JK, Stephens M, Donnelly P (2000) Inference of population structure using multilocus genotype data. *Genetics* 155(2):945–959.
34. Jensen JL, Bohonak AJ, Kelley ST (2005) Isolation by distance, web service. *BMC Genet* 6:13.
35. Rozas J (2009) DNA sequence polymorphism analysis using DnaSP. *Methods Mol Biol* 537:337–350.